An Improved Solid Lubricant for Bearings Operating in Space and Terrestrial Environments

Arindam Paul*, Harpal Singh*†, Kalyan C. Mutyala*‡ and G.L. Doll*

Abstract

The lubricity and durability of molybdenum disulfide (MoS_2) is controlled by the interfilm sliding and intrafilm flow. The primary reason for its ability to reduce friction is attributed to its crystal structure, which allows easy shearing of MoS_2 layers. Effective lubrication has been achieved under vacuum and dry conditions by employing MoS_2 as a solid lubricant. However, under humid conditions, the tribological performance of MoS_2 deteriorates. The deterioration can be offset through the incorporation of certain elements in MoS_2, which can also improve its tribological and mechanical properties. Demands on robustness and reliability provide motivations for improvements to broaden the application range of MoS_2 coatings in mechanical systems. Although Ti-MoS_2 coatings have been shown to perform extremely well in rolling contact, it is instructive to compare the tribological performance of this coating to MoS_2 and MoS_2 doped with Sb_2O_3 and Au, in sliding contact applications. Results of this investigation indicate that the Ti-MoS_2 coating outperforms MoS_2 and MoS_2 doped with Sb_2O_3 and Au in reciprocating sliding contact experiments performed in laboratory air at 30°C and 100°C.

Introduction

Solid lubricants are materials that can reduce friction between two surfaces sliding against each other without the use of a liquid media. Solid lubricants such as MoS_2 have been successfully utilized to reduce friction and wear in vacuum applications where liquid lubricants cannot be employed. MoS_2-based coatings are used as solid lubricants in various applications on earth and space such as cutting tools, gears, bearings, actuators and slip rings, among many others [1-3]. The tendency of MoS_2 to re-orient, from an initially random orientation, to a state where the {002} basal planes orient parallel to the surface is believed to be the major reason for its success as a solid lubricant [4, 5]. MoS_2 has a hexagonal crystal structure (D_{4h}^6 – $P6_3/mmc$) with a low friction coefficient due to the ease of its basal plane shearing. Basal planes have strong covalent bonds between S-Mo-S and weak van der Waals bonds between the planes. However, MoS_2 is susceptible to humid environments due to reactive edge sites that inhibit basal plane shearing and thereby increase its friction coefficient in the presence of oxygen and moisture [6]. Various elements (such as Ti, Cr, Zr, Au, Pb and Ni) and oxides (SbO_X, PbO) have been incorporated into MoS_2 coatings to improve their tribological performance [7–12]. The addition of metals or oxides greatly affects the tribological, mechanical and structural properties of MoS_2 composite coatings [13,14].

Ti and Sb_2O_3/Au doped MoS_2 coatings have found their way into several aerospace applications. The hardness and Young's modulus of doped MoS_2 is much higher than sputter-deposited MoS_2. The improvement in mechanical properties, load bearing capacity, and wear resistance over pure MoS_2 has also been attributed to the dopant content [1]. Recently, a Ti-MoS_2 coating was developed for rolling contact applications [4]. Although this particular coating was found to perform excellently as a solid lubricant material for rolling element bearings operating in laboratory air and vacuum testing, it was also found to greatly enhance fatigue life of rolling contact applications that operate in lubricated conditions [12]. Although the friction and wear of these coatings have been extensively studied using unidirectional and reciprocating sliding, it is beneficial to compare the tribological performances of several varieties of MoS_2 coatings that are deposited similarly. In this study, Ti-containing, Sb_2O_3/Au-containing, and pure MoS_2 coatings were

* Timken Engineered Surfaces Laboratory, University of Akron, Akron, OH

† Currently at Sentient Science, West Lafayette, IN

‡ Currently at Argonne National Laboratory, Lemont, IL

sputter-deposited on steel test coupons and their tribological performance was studied in humid air at two temperatures. The objective of this study was to determine the wear rates of the coatings and the wear rates of the uncoated, steel counter-faces.

Experimental Procedure

Deposition

Coatings were deposited onto AISI 52100 steel specimens in a high-vacuum, magnetron sputtering system. Ti and Sb_2O_3/Au targets were co-sputtered with MoS_2, a description of which can be found elsewhere [4], [6]. Singh et al. [4] described the deposition procedure and parameters in detail for the Ti-MoS_2 coating. All three coating depositions followed the same basic procedure. After ultrasonically cleaning the substrates in isopropyl alcohol, the substrates for the Ti-MoS_2 and MoS_2 coatings were placed onto a stationary fixture that faced two 50-mm-diameter magnetrons. First, the substrates were sputter etched with Ar ions for about 30 minutes. This removed surface contaminants and some of the native oxide from the steel specimens. Next, about 100 nm of Ti was deposited onto the substrates to form metallurgical bonds to the steel as well as to the functional coating. Different combinations of target materials were used in the deposition of the functional top layers of the three coating architectures. Only MoS_2 targets were sputtered to form the functional top layer of the undoped MoS_2 coating specimens, while both Ti and MoS_2 targets were sputtered simultaneously to form the functional top layer of the Ti-doped MoS_2 coating specimens. The functional top layer of the Sb_2O_3/Au-doped MoS_2 coating was deposited by simultaneously sputtering MoS_2 and Sb_2O_3/Au targets.

Characterizations

All three coatings were determined to be 1.1 ± 0.2 μm thick by means of the calotest procedure. Adhesion strengths of the coatings to their substrates were qualitatively determined to be excellent according to the standard Rockwell C indentation tests (DIN CEN/TS 1071-18). Whereas the Ti-MoS_2 and Sb_2O_3/Au-MoS_2 functional top layers have been determined previously to be amorphous by transmission electron microscopy, the undoped MoS_2 functional top layer was found to comprise randomly oriented, micro-crystallites of MoS_2. Compositional measurements performed by x-ray photoelectron spectroscopy indicated that all three functional top layers were slightly sub-stoichiometric in sulfur, and the dopant concentrations were about 18% and 15% for the Ti-MoS_2 and Sb_2O_3/Au-MoS_2 top layers, respectively.

Surface roughness measurements of the coatings were performed by 3D optical interferometry. The rms roughness values for the MoS_2, Sb_2O_3/Au-MoS_2, and Ti-MoS_2 coatings were determined to be 9 ± 1 nm, 7 ± 2 nm, and 8 ± 2 nm, respectively. The average rms roughness values of the uncoated AISI 52100 balls was 598 ± 19 nm.

Tribological Test Parameters

Dry reciprocating sliding contact experiments were performed on a ball on disk tribometer at a contact stress of 660 MPa (96 ksi). These tests were conducted with a sliding amplitude of 1 mm, a frequency of 20 Hz, and a normal load of 1 N. Tests were conducted in laboratory air (17% RH) and at 30°C and 100°C. Coefficients of friction were determined in situ, and at least 3 different durations (sliding distances) were performed for each temperature. Subsequent to each test, wear scars in the coatings and on the uncoated balls were measured using 3D optical profilometry. Wear volumes for the steel balls and coated disks were determined as a function of dissipated energy (E_d), where E_d is the product of the frictional force and the sliding distance. Although wear volumes of the coating were determined directly using 3D optical interferometry, wear volumes of the balls were calculated from a measurement of the radius of the wear scar

$$V_{ball} = \frac{\pi h}{6}(h^2 + 3r^2) \quad (1)$$

where

$$h = R_b - \sqrt{R_b^2 - r^2} \quad , \quad (2)$$

R_b is the radius of the ball [μm], and r is the radius of the wear scar [μm].

Results

MoS_2

Average friction coefficients (μ_{avg}) with standard deviations measured for the three coatings at 30°C and at 100°C are displayed in Figure 1. The three values of μ_{avg} at 30°C for steel paired with MoS_2, Sb_2O_3/Au-MoS_2 and Ti-MoS_2 are 0.19 ± 0.03, 0.21 ± 0.04, and 0.20 ± 0.01, respectively and are statistically equivalent. Average friction coefficients for the 100°C tests are 0.09 ± 0.01, 0.04 ± 0.00, and 0.09 ± 0.03 for steel paired with MoS_2, Sb_2O_3/Au-MoS_2 and Ti-MoS_2, respectively. Notably, μ_{avg} corresponding to the Sb_2O_3/Au-MoS_2 pairing is about 50% less than the values obtained for the Ti-MoS_2 and MoS_2 pairings. The low value of μ_{avg} for the Sb_2O_3/Au-MoS_2 coating has been attributed to thermally driven Ostwald ripening of the Ag and subsequent diffusion of agglomerated Ag to the Sb_2O_3/Au-MoS_2 surface [6].

Wear volumes (V) for the MoS_2 coating and mated steel ball obtained from tests performed at 30°C are displayed and plotted against E_d in Figure 2 along with optical images of the wear scars generated after 17,000 cycles. Lines in the figures are least square fits of

$$\boldsymbol{V = \alpha E_d + V_o} \tag{3}$$

where α is the wear coefficient $\mu m^3/J$, E_d is the dissipated energy J, and Vo is the offset μm^3. The values of R^2 close to unity indicate the goodness of the fits. The wear coefficients for the ball and the MoS_2 coating were determined to be 772 ± 26 $\mu m^3/J$ and 3282 ± 10 $\mu m^3/J$, respectively.

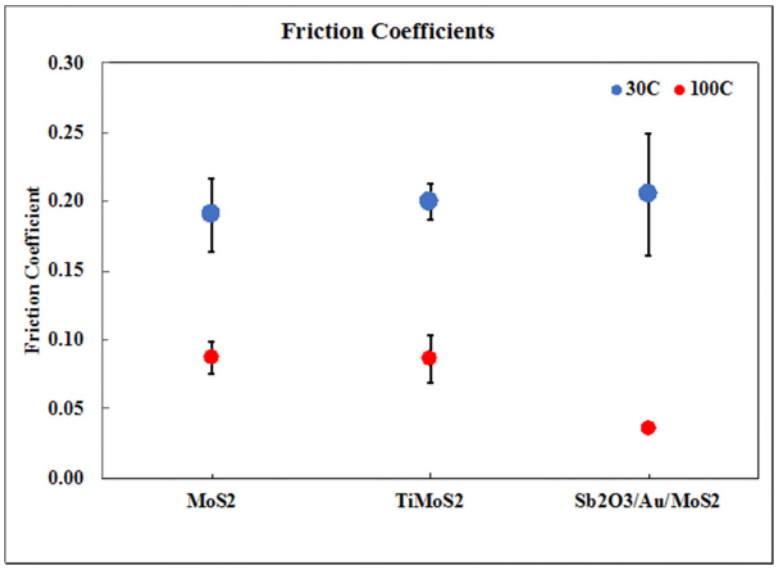

Figure 1. Average friction coefficients and standard deviations for the three coatings at 30°C and 100°C obtained in reciprocating sliding contact with a sliding amplitude of 1 mm, a frequency of 20 Hz, and a contact stress of 660 MPa.

Wear volumes for the MoS_2 coating and mated steel balls obtained from tests performed at 100°C are displayed and plotted against E_d in Figure 3 along with optical images of the wear scars generated after 17,000 cycles. The wear coefficients for the ball and the MoS_2 coating for tests performed at 100°C were determined to be 719 ± 56 $\mu m^3/J$ and 12,832 ± 747 $\mu m^3/J$, respectively. The 100°C wear coefficient of the MoS_2 is about four times that associated with the 30°C results.

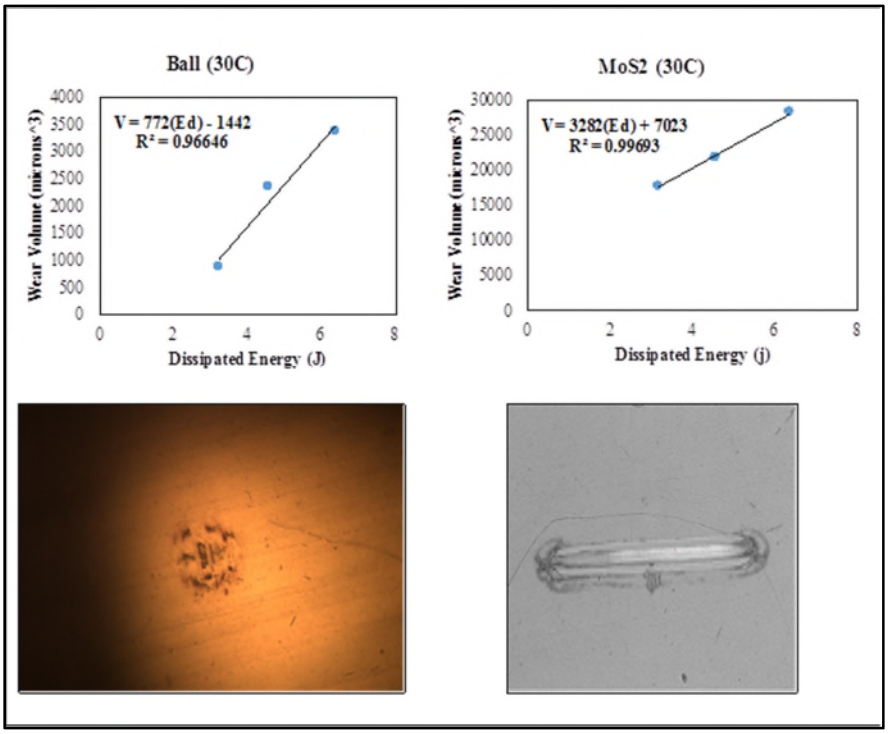

Figure 2. Wear volumes (V) for the MoS_2 coating and mated steel ball obtained from tests performed at 30°C are plotted against E_d along with optical images of the wear scars on the ball and coating generated after 17,000 cycles. Lines in the figures are least square fits of Eq. 3 to the data.

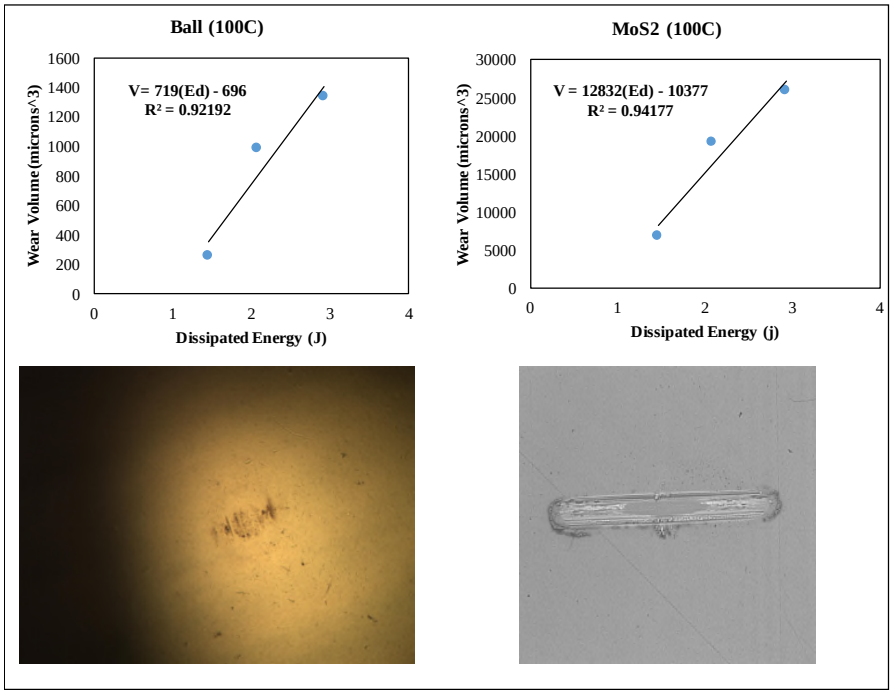

Figure 3. Wear volumes (V) for the MoS_2 coating and mated steel ball obtained from tests performed at 100°C are plotted against E_d along with optical images of the wear scars on the ball and coating generated after 17,000 cycles. Lines in the figures are least square fits of Eq. 3 to the data.

Inspection of the optical images of the ball and MoS_2 in Figure 3 provides support for the wear results. That is, the very small wear scar on the ball contains less transferred material than the ball wear scar in Figure 2, and the wear scar on the MoS_2 coating in Figure 3 is deeper than that in Figure 2. In fact, the image of the MoS_2 wear scar may show an elliptical patch of the substrate or the Ti interlayer in the center of the scar.

Sb_2O_3/Au-MoS_2

Wear volumes (V) for the Sb_2O_3/Au-MoS_2 coating and mated steel ball obtained from tests performed at 30°C are displayed and plotted against E_d in Figure 4 along with optical images of the wear scars generated after 17,000 cycles. The wear coefficients for the ball and the Sb_2O_3/Au-MoS_2 coating for tests performed at 30°C were determined to be 17,000 ± 3,000 $\mu m^3/J$ and 4,233 ± 194 $\mu m^3/J$, respectively. The optical image of the ball shows an extremely large wear scar with isolated islands of transferred material, which is consistent with the large value of the wear coefficient. On the other hand, the wear scar produced on the Sb_2O_3/Au-MoS_2 coating is relatively shallow.

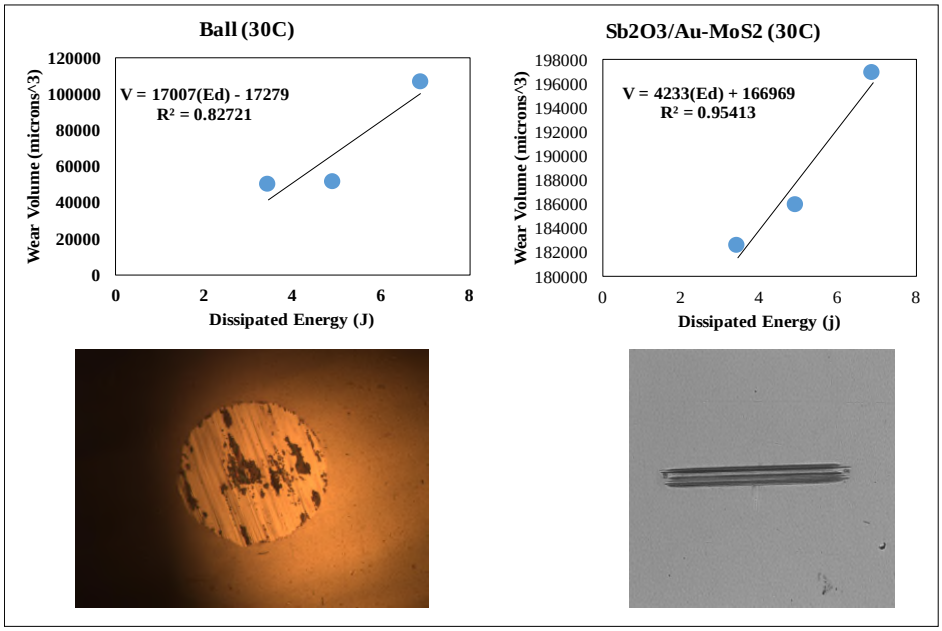

Figure 4, Wear volumes (V) for the Sb_2O_3/Au-MoS_2 coating and mated steel ball obtained from tests performed at 30°C are plotted against E_d along with optical images of the wear scars on the ball and coating generated after 17,000 cycles. Lines in the figures are least square fits of Eq. 3 to the data.

Figure 5 displays the wear volumes for the Sb_2O_3/Au-MoS_2 coating and mated steel ball obtained from tests performed at 100°C. The wear coefficients for the ball and the Sb_2O_3/Au-MoS_2 coating were determined to be 2187 ± 6 $\mu m^3/J$ and 5,032 ± 386 $\mu m^3/J$, respectively. The image of the wear scar on the Sb_2O_3/Au-MoS_2 coating displays a very shallow depth without a debris field surrounding the scar. The ball wear scar radius is very small and the scar is well-covered by a transfer film. The absence of a debris field suggests that the majority of the coating that was worn in the test, became a transfer film on the ball. This is an indication that the Sb_2O_3/Au-MoS_2 coating formed an effective VAL during the 100°C test.

Ti-MoS_2

Wear volumes for the Ti-MoS_2 coating and mated steel ball obtained from tests performed at 30°C are displayed and plotted against E_d in Figure 6 along with optical images of the wear scars generated after 17,000 cycles. The wear coefficients for the ball and the Ti-MoS_2 coating for tests performed at 30°C were determined to be 290 ± 89 $\mu m^3/J$ and 10,816 ± 894 $\mu m^3/J$, respectively. The optical image of the ball shows a moderate wear scar with an almost complete coverage of transferred material, which is consistent with the small value of the wear coefficient. The wear scar produced on the Ti-MoS_2 coating is relatively shallow and does not exhibit a large debris field. This indicates that the majority of the coating that was worn in the

test wound up as a transfer film on the ball. This is an indication that the Ti-MoS2 coating formed an effective VAL during the 30°C test.

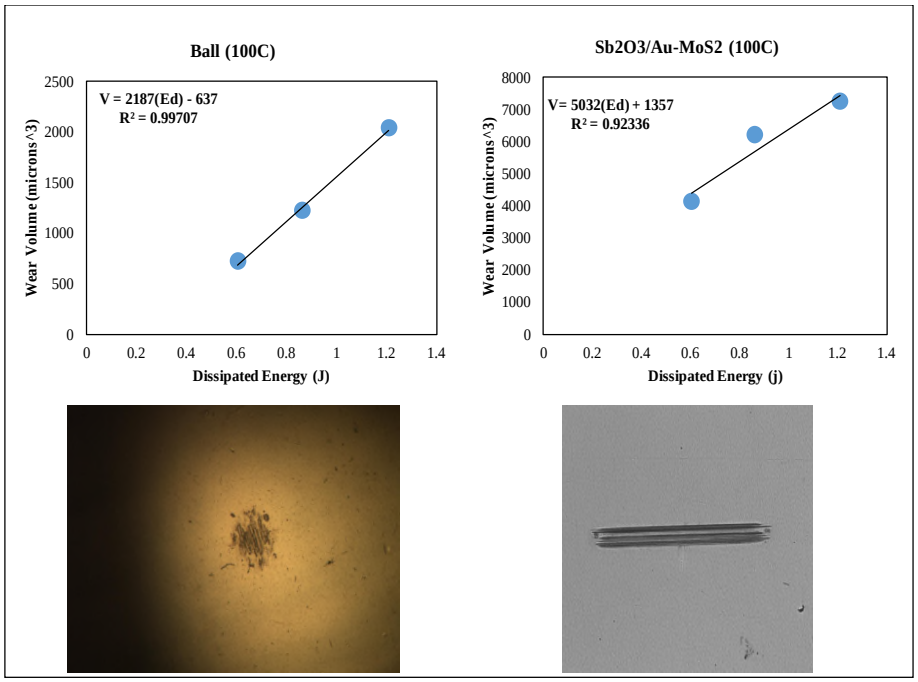

Figure 5, Wear volumes (V) for the Sb_2O_3/Au-MoS_2 coating and mated steel ball obtained from tests performed at 100°C are plotted against E_d along with optical images of the wear scars on the ball and coating generated after 17,000 cycles. Lines in the figures are least square fits of Eq. 3 to the data.

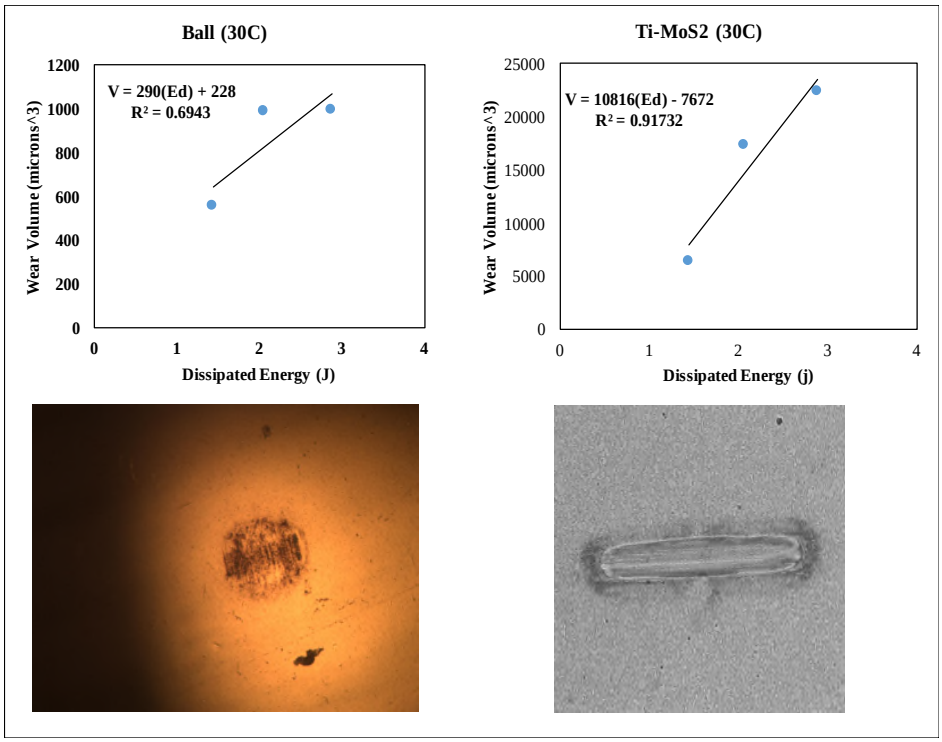

Figure 6, Wear volumes (V) for the Ti-MoS_2 coating and mated steel ball obtained from tests performed at 30°C are plotted against E_d along with optical images of the wear scars on the ball and coating generated after 17,000 cycles. Lines in the figures are least square fits of Eq. 3 to the data.

Figure 7 displays the wear volumes for the Ti-MoS_2 coating and mated steel ball obtained from tests performed at 100°C. The wear coefficients for the ball and the Ti-MoS_2 coating were determined to be 1,438 ± 16 mm^3/J and 7,941 ± 222 mm^3/J, respectively. The optical image of the ball shows a moderate wear scar radius with complete coverage of transferred material, which is consistent with the small value of the wear coefficient. The wear scar produced on the Ti-MoS_2 coating is relatively shallow and does not exhibit a large debris field. This indicates that the majority of the coating that was worn in the test wound up as a transfer film on the ball, and an indication that the Ti-MoS_2 coating also formed an effective VAL during the 100°C test.

Discussion

Ball and coating wear coefficients determined from analysis of the 30°C and 100°C data are gathered in Table 1. It is convenient to assign wear regimes as low (α_L < 1000 $\mu m^3/J$), moderate (1000 $\mu m^3/J$ < α_M < 10,000 $\mu m^3/J$), and high (α_H > 10,000 $\mu m^3/J$). According to this convention, low ball wear rates were obtained for the 30°C measurements from the Ti-MoS_2 and MoS_2 coatings, with the lowest ball wear rate produced by the Ti-MoS_2 coating. An extraordinarily high ball wear rate was produced by the Sb_2O_3/Au-MoS_2 coating during the 30°C test. Whereas the 30°C measurements generated moderate wear rates on the Sb_2O_3/Au-MoS_2 and MoS_2 coatings, the wear rate of the Ti-MoS_2 just falls in the high wear category. The MoS_2 coating had the lowest wear rate at 30°C.

The MoS_2 coating produced the lowest ball wear rate of the 100°C tests, while the Ti-MoS_2 and the Sb_2O_3/Au-MoS_2 coatings generated moderate ball wear rates. Of the coating wear rates at 100°C, the Ti-MoS_2 and the Sb_2O_3/Au-MoS_2 coatings had moderate wear rates while the MoS_2 coating had a high wear rate.

The Sb_2O_3/Au-MoS_2 coating exhibited a high degree of abrasiveness to the steel ball. Incorporation of the Sb_2O_3 in the MoS_2 is believed to disrupt the ability of the material to achieve long range crystallographic order, making the coating less susceptible to degradation from moisture [10]. The proposed mechanism through which this coating can achieve a sustainable VAL is by the thermally driven diffusion of Ag to the surface of the coating [6]. It is proposed that the average friction coefficient of μ_{avg} = 0.2 measured in the 30°C experiments was insufficient to generate enough local heating of the coating to initiate Ag diffusion. Furthermore, it is also proposed that the Sb_2O_3 content in the coating was responsible for the abrasiveness exhibited during the 30°C testing. On the other hand, the coating was much less abrasive in the 100°C tests and the pairing with the steel ball yielded a very small friction coefficient of m_{avg} = 0.04. This appears to indicate that the elevated temperature of 100°C was sufficient to establish a beneficial VAL between the steel and this coating.

An effective VAL is one that inhibits high amounts of wear of the coating and the counterface over the temperature range and relative motion experienced by a specific application. Although Ti-MoS_2 has been previously shown to perform exceptionally well in rolling contact [4,9,12], based upon the results of these measurements, it can be concluded that the Ti-MoS_2 coating would meet the VAL requirements better than the tested MoS_2 and Sb_2O_3/Au-MoS_2 coatings when in contact with reciprocating sliding steel counterfaces over a temperature range of 30°C to 100°C.

It is important to point out that although the experiments were performed in laboratory air, the environment had a very low humidity (17% RH) during the testing. Although it is expected that the wear rates of all three coatings will increase with increasing relative humidity, undoped MoS_2 tends to experience the greatest increase [3].

Table 1: Wear rates in [mm³/J] determined for the mated ball and coatings tested at 30°C and 100°C.

Coating	**30°C**		**100°C**	
	Ball Wear [$\mu m^3/J$]	Coating Wear [$\mu m^3/J$]	Ball Wear [$\mu m^3/J$]	Coating Wear [$\mu m^3/J$]
MoS_2	772 ± 326	3,282 ± 10	719 ± 56	12,832 ± 747
Sb_2O_3/Au-MoS_2	17,007 ± 2,939	4,233 ± 194	2,187 ± 6	5,032 ± 386
Ti-MoS_2	290 ± 89	10,816 ± 894	1,438 ± 16	7,941 ± 222

Conclusions

Some aerospace applications such as rolling element bearings and gears have utilized MoS_2 and Sb_2O_3/Au-MoS_2 solid lubricant coatings in demanding environments where conventional oils or greases are unsuitable. Results of this study combined with the results of previous studies [4,9,12], strongly indicate that Ti-MoS_2 merits consideration as a solid lubricant coating for rolling element bearing and gearing applications. Important findings of this study include:

- Whereas the MoS2 coating performed well at 30°C, it experienced a high wear rate at 100°C and failed to form a VAL in the contact with a steel counterface.
- The Sb_2O_3/Au-MoS_2 coating required an elevated temperature of 100°C to form a VAL, and was extremely abrasive to the steel counterface at 30°C.
- The Ti-MoS2 coating formed effective VALs at 30°C and 100°C.

Acknowledgements

The authors are thankful to The Timken Company for providing financial support and guidance for this project. The authors appreciate the help of Dr. Barbara Fowler of Timken Engineered Surface Laboratories for her help in tribological testing and characterization analysis, and Haifeng Qin (UA Chemical and Biomolecular Engineering) and Zhencheng Ren (UA Mechanical Engineering) for their assistance with the deposition system. The authors also thank Dr. Ryan Evans from The Timken Company, Dr. Hamidreza Mohseni (now at Bosch) and Prof. Thomas Scharf at the University of North Texas for past contributions.

References

1. Teer, D. G. "New solid lubricant coatings." *Wear* 251.1-12 (2001): 1068-1074.
2. Hilton, Michael R., et al. "Structural and tribological studies of MoS_2 solid lubricant films having tailored metal-multilayer nanostructures." *Surface and Coatings Technology* 53.1 (1992): 13-23.
3. Sliney, Harold E. "Solid lubricant materials for high temperatures—a review." *Tribology International* 15.5 (1982): 303-315.
4. Singh, H., et al. "Tribological performance and coating characteristics of sputter-Deposited Ti-Doped MoS_2 in rolling and sliding contact." *Tribology Transactions* 58.5 (2015): 767-777.
5. Singer, I. L., et al. "Role of third bodies in friction and wear of protective coatings." *Journal of Vacuum Science & Technology A: Vacuum, Surfaces, and Films* 21.5 (2003): S232-S240.
6. Scharf, T. W., P. G. Kotula, and S. V. Prasad. "Friction and wear mechanisms in MoS2/Sb_2O_3/Au nanocomposite coatings." *Acta Materialia* 58.12 (2010): 4100-4109.

7. Singh, H., et al. "An investigation of material and tribological properties of Sb_2O_3/Au-doped MoS_2 solid lubricant films under sliding and rolling contact in different environments." *Surface and Coatings Technology 284* (2015): 281-289.
8. Stupp, Bernard C. "Synergistic effects of metals co-sputtered with MoS_2." *Thin solid films* 84.3 (1981): 257-266.
9. Singh, H., et al. "Tribological performance and coating characteristics of sputter-Deposited Ti-Doped MoS_2 in rolling and sliding contact." *Tribology Transactions* 58.5 (2015): 767-777.
10. Singh, Harpal, et al. "An atom probe tomography investigation of Ti–MoS_2 and MoS_2–Sb_2O_3–Au films." *Journal of Materials Research* 32.9 (2017): 1710-1717.
11. Pope, L. E., and J. K. G. Panitz. "The effects of hertzian stress and test atmosphere on the friction coefficients of MoS_2 coatings." *Surface and Coatings Technology* 36.1-2 (1988): 341-350.
12. Mutyala, Kalyan C., et al. "Deposition, characterization, and performance of tribological coatings on spherical rolling elements." *Surface and Coatings Technology* 284 (2015): 302-309.
13. Stoyanov, Pantcho, et al. "Microtribological performance of Au–MoS_2 and Ti–MoS_2 coatings with varying contact pressure." *Tribology letters* 40.1 (2010): 199-211.
14. Windom, Bret C., W. G. Sawyer, and David W. Hahn. "A Raman spectroscopic study of MoS_2 and MoO_3: applications to tribological systems." *Tribology Letters* 42.3 (2011): 301-310.
15. Berthier, Y., M. Godet, and M. Brendle. "Velocity accommodation in friction." *Tribology Transactions* 32.4 (1989): 490-496.
16. Godet, Maurice. "Third-bodies in tribology." *Wear* 136.1 (1990): 29-45.